Title

Intrinsic cholinergic innervation in the human sigmoid colon revealed using CLARITY, three-dimensional (3D) imaging, and a novel anti-human peripheral choline acetyltransferase (hpChAT) antiserum

Journal

Neurogastroenterology & Motility, 33(4)

ISSN

1350-1925

Authors

Yuan, Pu-Qing
Bellier, Jean-Pierre
Li, Tao
et al.

Publication Date

2021-04-01

DOI

10.1111/nmo.14030

Peer reviewed

HHS Public Access

Author manuscript

Neurogastroenterol Motil. Author manuscript; available in PMC 2021 May 16.

Published in final edited form as:

Neurogastroenterol Motil. 2021 April ; 33(4): e14030. doi:10.1111/nmo.14030.

Intrinsic cholinergic innervation in the human sigmoid colon revealed using CLARITY, three-dimensional (3D) imaging, and a novel anti-human peripheral choline acetyltransferase (hpChAT) antiserum

Pu-Qing Yuan[1,2], **Jean-Pierre Bellier**[3], **Tao Li**[1], **Mary R. Kwaan**[4], **Hiroshi Kimura**[3], **Yvette Taché**[1,2]

[1]CLA/Digestive Diseases Research Core Center, Vatche and Tamar Manoukian Digestive Diseases Division, Department of Medicine, UCLA David Geffen School of Medicine, Los Angeles, CA, USA

[2]VA Greater Los Angeles Healthcare System, Los Angeles, CA, USA

[3]Molecular Neuroscience Research Center, Shiga University of Medical Science, Otsu, Japan

[4]Department of Surgery, UCLA David Geffen School of Medicine, Los Angeles, CA, USA

Abstract

Background: We previously reported the specificity of a novel anti-human peripheral choline acetyltransferase (hpChAT) antiserum for immunostaining of cholinergic neuronal cell bodies and fibers in the human colon. In this study, we investigate 3D architecture of intrinsic cholinergic innervation in the human sigmoid colon and the relationship with nitrergic neurons in the enteric plexus.

Methods: We developed a modified CLARITY tissue technique applicable for clearing human sigmoid colon specimens and immunostaining with hpChAT antiserum and co-labeling with neuronal nitric oxide synthase (nNOS) antibody. The Z-stack confocal images were processed for 3D reconstruction/segmentation/digital tracing and computational quantitation by Imaris 9.2 and 9.5.

Key Results: In the mucosa, a local micro-neuronal network formed of hpChAT-ir fibers and a few neuronal cell bodies were digitally assembled. Three layers of submucosal plexuses were displayed in 3D structure that were interconnected by hpChAT-ir fiber bundles and hpChAT-ir neurons were rarely co-labeled by nNOS. In the myenteric plexus, 30.1% of hpChAT-ir somas including Dogiel type I and II were co-labeled by nNOS and 3 classes of hpChAT-ir nerve fiber

Correspondence: Pu-Qing Yuan, CURE: DDRC, VA GLAHS, Bldg. 115, Rm. 107A, 1301 Wilshire Blvd., Los Angeles, CA 90073, USA. pqyuan@mednet.ucla.edu.

AUTHOR CONTRIBUTIONS

Design the study: PQY, YT; performed the experiments: PQY, TL; contributions to the methodology: PQY, JPB, MRK, HK. Wrote the manuscript: PQY, YT. Give input on the written manuscript; HK, JPB, MRK. All authors listed provide approval for publication.

CONFLICT OF INTEREST

HK and JPB have a patent pending (Japanese 04412018). Antibody for detecting human peripheral cholinergic nerve (2018).

SUPPORTING INFORMATION

Additional supporting information may be found online in the Supporting Information section.

strands were visualized in 3D images and videos. The density and intensity values of hpChAT-ir fibers in 3D structure were significantly higher in the circular than in the longitudinal layer.

Conclusions and Inferences: The intrinsic cholinergic innervation in the human sigmoid colon was demonstrated layer by layer for the first time in 3D microstructures. This may open a new venue to assess the structure-function relationships and pathological alterations in colonic diseases.

Keywords

3D imaging; cholinergic innervation; enteric nervous system; human sigmoid colon; nitric oxide synthase

1 | INTRODUCTION

The enteric nervous system (ENS) in most regions of the human gut consists of two main ganglionated layers: the myenteric plexus (MP) that lies between the longitudinal and circular layers of muscularis externa (ME) and the submucosal plexuses (SMP) within the submucosa.[1–3] The ENS in the intestine is endowed of complex reflex circuits that play a role in controlling several functions including motility, fluid exchange between the lumen and mucosa and local blood flow.[4] A detailed visualization of the three-dimensional (3D) architecture and topography of ENS in its spatial environment will extend knowledge of structure-function relationships. However, the heterogeneous optical properties and mismatched refractive index among different components within the human colon tissue scatter the incoming light and restrict large volume imaging with microscopic resolution.[5,6] Therefore, new innovative methodological approaches for 3D mapping of projections and connections of the human ENS network are required.

A tissue clearing technique called CLARITY (Clear Lipid-exchanged Acrylamide-hybridized Rigid Imaging/Immunohistochemistry/In situ-hybridization-compatible Tissue-hYdrogel) has been recently developed to produce transparent tissue without quenching endogenous fluorescence thereby offering a unique method for imaging intact whole-tissue specimens.[7,8] This technique not only preserves spatial relationships and tissue microstructures by forming a tissue-hydrogel hybrid with increased permeability for deep optical interrogation, but also enables immunofluorescence and maintenance of fluorophores during imaging of large volumes for 3D reconstruction and mapping.[9] Therefore, this approach has been successfully used in rodents for clearing organs such as the brain, heart, pancreas, stomach, and kidney.[10–14] However, it is less applied to human tissues, particularly the human colon which contains large amount of light-scattering lipids and thick fibrous components.[15]

Acetylcholine (ACh) is one of the major neurotransmitters in the ENS excitatory motor neurons and interneurons.[16] Results of functional and electrophysiological studies indicate the significance of cholinergic excitatory mechanisms for transmission within the ENS and for the innervation of both muscle and secretory cells.[17] In particular, the sigmoid colonic motility changes induced by ACh mimicked the functional sigmoid response in patients with

diarrhea[18] and this segment can be affected by benign diseases.[19] However, still little is known about the cholinergic innervation of the human sigmoid colon.

The main objective of this study was to fill up the gap in anatomical mapping of the intrinsic cholinergic innervation of the human sigmoid colon, particularly in 3D structures. To this end, firstly, we developed a modified CLARITY protocol adapted to tissue properties of human sigmoid colon and compatible with immunofluorescence using a recently characterized mouse anti-human peripheral ChAT (hpChAT) protein antiserum.[20] This antiserum labels peripheral cholinergic nerve cell bodies and fibers in the human large intestine without cross-reacting with the common ChAT expressed in the central nervous system (CNS).[20] Secondly, we reconstructed 3D images from Z-stacks of confocal images and traced digitally the local process projections and connectivity of hpChAT immunoreactive (ir) neurons in the SMP and MP using Imaris 9.2 and 9.5 for neuroscientist. Then, the density and intensity of hpChAT-ir fibers innervating the circular and longitudinal muscle layers were computationally quantitated and compared. Lastly, we determined the co-localization of hpChAT and neuronal nitric oxide synthase (nNOS) by using Imaris 9.5 spot function within layers of enteric plexuses to assess the distribution of known excitatory and inhibitory motor pathways.[21]

2 | MATERIALS AND METHODS

2.1 | Human sigmoid colon

The post-operative samples of the sigmoid colon were collected from four patients (two females, two males, median age 45 years old, range 38–58 years) with colonic adenocarcinoma or history of diverticulitis. None of the patients had active colonic infections when the tissues were sampled. The full thickness healthy margin of colonic specimens (about 5 × 3 cm) was provided by the University of California at Los Angeles (UCLA) Translational Pathology Core Laboratory after dissection and examination to be normal under macro- and microscopic inspection. Samples were immersed in Belzer UW® Cold Storage Solution (Bridge to Life Ltd, Columbia, SC) on ice to be processed for CLARITY. The interval time between the resection of the colon and the beginning of CLARITY was 70–90 min. The use of human colon tissues was approved by UCLA Institutional Review Board for Biosafety and Ethics (IRB #17–001686). Informed consent has been obtained in all cases.

2.2 | CLARITY

The protocol of passive CLARITY for brain[7] was modified for clearing the human sigmoid colon. Briefly, samples were pinned-flat on the Sylgard-coated dishes, immersed in an ice-cold hydrogel solution containing a mixture of 4% paraformaldehyde (Sigma-Aldrich, St Louis, MO), 4% acrylamide 0.05% bisacrylamide (BIO-RAD, Hercules, CA) and 0.25% VA044 (Wako, Richmond, VA) in phospate-buffered saline (PBS) and maintained at 4°C overnight for hydrogel-tissue hybridization. On the second day, flat samples were cut in small pieces (1 × 1 cm) and kept at 4°C for at least 2–3 days in the hydrogel solution. Then, they were transferred to 50 ml conical tubes containing 15 ml of fresh hydrogel solution to replace all oxygen (known to inhibit the acrylamide polymerization) with pure nitrogen gas.

The hydrogel polymerization was initiated by submerging the conical tubes with tissue samples in a temperature-controlled 37°C water bath (Precision Scientific Water Bath Model 182, Thermo Scientific, Marietta, OH) for 3 h until the hydrogel solution no longer flowed and had polymerized. Pieces of samples (6–8) were separated into submucosa (SM) and muscularis externa (ME) after the mucosa was peeled off. The excess hydrogel monomers were washed out from inside the SM and ME on a shaker/rotator plate (70 rpm, New Brunswick Scientific Co., Edison, NJ) with a clearing solution containing 6% sodium dodecyl sulfate (SDS) (Sigma-Aldrich) in sodium borate buffer (200 mM, pH 8.5) (Sigma-Aldrich) at 37°C for 3–4 weeks until clearing is achieved. Thereafter, samples were placed in 0.1% Triton-X 100 (Sigma-Aldrich) in PBS (TPBS) on a shaker/rotator plate for 2 days (37°C, 70 rpm) to wash out SDS micelles. Other 2 pieces with full layers were cut into 0.5–1 mm vertical sections using a vibratome (Campden Instruments LTD, Lafayette, IN) after hydrogel polymerization followed by washing with clearing solution as described above for 1–2 weeks. This additional approach enabled us to visualize simultaneously the colonic innervation in different layers and connections among them and accelerated the clearing procedure as well.

2.3 | Immunohistochemistry

CLARITY-cleared samples were transferred into Corning™ Costar™ Flat Bottom 24 Well Plates (Fisher Scientific, Hampton, NH). All antibody incubations and washing steps were conducted with gentle shaking (90 rpm, Corning™ LSE™ Low Speed Orbital Shaker, Fisher Scientific, Canoga Park, CA). After immersion in 10% normal donkey serum in TPBS at room temperature (RT) for one day to block nonspecific interactions and to enhance permeabilization, samples were incubated in primary antibodies (Table 1). The antibody protein gene product 9.5 (PGP9.5), a pan-neuronal marker,[22] was used as a counterstain to display all neuronal components. To further characterize the specificity of the novel hpChAT antiserum in labeling of human colonic enteric cholinergic neurons,[20] double labeling was performed with hpChAT antiserum and other two classic ChAT antibodies: a goat anti-human ChAT antibody from Chemicon (AB144p) or a rabbit anti-porcine ChAT antibody from Dr. Michael Schemann (P3YEB). These two antibodies represented the most popular ChAT antibodies commonly used to label human enteric cholinergic neurons.[23,24] To determine the co-localization of hpChAT and nNOS, a nitrergic neuronal marker,[25,26] double immunolabeling was carried out with a cocktail of mouse hpChAT antiserum and rabbit nNOS antibody. The primary antibody incubation was processed at RT for 2 days for vertical sections or at RT for 1 day followed by 4 days at 4°C for SM and ME preparations. After washing with PBS at RT for 1 day, samples were incubated in fluorescence labeled secondary antibodies (Table 1) on a shaker at RT with shaking for 1 day and then washed with PBS at RT for 1 day. Negative control samples were subjected to the same procedures without primary antibody. Samples were then immersed in a custom-made refractive index matching solution (RIMS) containing 88% Histodenz (Sigma-Aldrich) in 0.02 M phosphate buffer with 0.01% sodium azide (pH 7.5) with a refractive index of 1.46 at 4°C[8] until transparent (1 day for 0.5–1 mm vertical sections, 2–3 days for 1 × 1 cm SMP and ME samples). Samples were mounted with fresh RIMS in a sealed watertight well prepared with iSpacers (SunJin Lab, Hsinchu City, Taiwan), which are made from different thickness adhesive tape.

2.4 | 3D Imaging and digital tracing

Images were acquired with Zeiss LSM 710 confocal microscopes (Carl Zeiss Microscopy, LLC, White Plains, NY). The Alexa 488 and Alexa 555 fluorophores were excited using a 488 nm Argon laser and a 561–10 nm diode-pumped solid-state laser, respectively. The Z-axis intervals were 1 μm with depths between 200 and 500 μm for SMP and ME, and 500 and 1000 μm for full layer vertical sections. The confocal parameters were determined, and the same setting was applied for each sample. The images were collected using Zen image collection software (Carl Zeiss Microscopy) and processed for 3D reconstruction, video generation, segmentation, digital tracing using Imaris 9.2 and 9.5 for Neuroscientists (Bitplane Inc., Concord, MA). User-guided fiber tracing and partial projections were used in 3D tracing mode. The special features and connections were confirmed by careful observations in higher magnification, rotation, and partial projections of layers.

2.5 | Quantitative and statistical analysis

The density and intensity of hpChAT-ir and PGP 9.5-ir fibers in the ME were computationally quantitated by using Imaris 9.5 for Neuroscientists on 3D images acquired from 0.5–1 mm vertical sections with full layers after passive CLARITY. Each 3D image was generated from 500–550 optical sections (Z-stack) with 1415 × 1415 μm frame and 1-μm apart (10× objective), and 5–6 images per patient were selected from 3 patients (one patient was not included due to its fragmentary longitudinal muscle layer). The entire circular and longitudinal muscle layers were contoured separately in each 3D image. Within the MeasurementPro module, the PGP9.5-ir and hpChAT-ir fibers were traced and their volumes were measured separately in the contoured muscle layers. The density of total nerve (PGP9.5-ir) and cholinergic (hpChAT-ir) fibers was expressed as percentage of fibers in the volume of contoured muscle layer ($\mu m^3/\mu m^3$, %). The intensity of immunofluorescence in the hpChAT-ir and PGP9.5-ir fibers was assessed using 488 and 555 nm channels separately. To reduce the possible error raised from sampling and staining at different times, the intensity measurement was performed simultaneously within the circular and longitudinal layers on the same image. Average intensity of immunofluorescence in the total volume of hpChAT-ir or PGP9.5-ir nerve fibers in each 3D image was calculated and expressed as arbitrary units/μm^3. hpChAT-ir or nNOS-ir enteric neurons were coded with Imaris 9.5 spot function in 3D images. The coded color spots (hpChAT or nNOS-ir neurons) were extracted and automatically counted within contoured ganglia. The number of coded color spots (hpChAT-ir or nNOS-ir neurons) per volume of ganglion (mm^3) was calculated in 4–10 ganglia in each plexus per patient ($n = 3$ for ISP and OSP, 4 for MP), respectively and expressed as percentage of hpChAT-ir or nNOS-ir neurons in total hpChAT +nNOS-ir neurons. The co-localization of hpChAT and nNOS was assessed in 4–10 ganglia per sample in each plexus by using Imaris “Center Point” mode. Two different color spots with a shortest distance between the centers within 10.5 μm were counted as colocalized neurons. A co-localization channel (yellow color) was created with the ImarisColoc tool to calculate the proportion of colocalized neurons in the hpChAT-ir or nNOS-ir neurons. Multiple group comparisons were performed with one-way analysis of variance (ANOVA) followed by Tukey’s *post hoc* test. A p value <0.05 was considered statistically significant.

3 | RESULTS

3.1 | Immunostaining of human colon cholinergic neurons: Comparison of hpChAT antiserum with two classic ChAT antibodies

The double labeling with mouse anti-hpChAT antiserum (Figure 1A,D) and goat anti-human ChAT (Chemicon, AB144p) (Figure 1B) or rabbit anti-porcine ChAT antibody (from Dr. Michael Schemann, P3YEB) (Figure 1E) demonstrated that the immunoreactivity of hpChAT overlapped fully with that of ChAT (AB144p) (Figure 1C) or mostly with ChAT (P3YEB) (Figure 1F) as shown on confocal microscope images created with Imaris 9.2 slice mode and taken from human sigmoid colon after modified passive CLARITY technique. Compared with ChAT (AB144p) (Figure 1B) and ChAT (P3YEB) (Figure 1E), hpChAT immunostaining provided a more intense, clearer and sharper neuronal profile, with more detailed structures and fine fibers with high resolution (Figure 1A,D). No immunoreactivity was observed in the preparations incubated with the antibody diluent alone instead of primary antibodies (data not shown).

3.2 | Tissue clearing and 3D imaging of cholinergic innervation in the sigmoid colon

Using the modified CLARITY protocol developed, the human sigmoid colon specimen with full thickness was cleared within 6–7 weeks making the grid lines visible through the completely transparent sample (Figure 2A,B). This allowed us to image deeply and obtain high quality confocal images of neuronal structures labeled with marker antibodies for 3D reconstruction.

3.2.1 | Mucosa—The 3D images and videos showed rich hpChAT-ir nerve fibers distributed in the mucosa projecting from submucosal neuronal cell bodies (Figure 2C, Video S1). These fine intrinsic cholinergic nerve fibers protruded into the lamina propria and surrounded the mucosal crypts forming a nerve network of honeycomb-like architecture (Figure 1D). A few hpChAT-ir nerve cell bodies with multidendritic and uniaxonal morphology were also observed at the intersections of nerve fiber strands in the lamina propria (Figure 2D).

3.2.2 | Muscularis externa (ME)—In the human sigmoid colon, the ME consists of two layers of smooth muscle: inner—circular and outer—longitudinal muscle and MP including nerve fiber network and neurons in the ganglia. The outer longitudinal layer of smooth muscle varies in thickness and forms three thick longitudinal bands, the taeniae coli. We selected the region between the tenia where the longitudinal muscle is thinner so that easier to facilitate antibody penetration and to perform optical scanning for 3D imaging. Cholinergic nerve fibers and ganglia were labeled by hpChAT in green (Figures 3A, 4B), and the pan-neuronal marker PGP9.5 was used to display all neuronal components in red (Figures 3B, 4C). In the merged image, most of nerve fiber bundles and ganglia were double-labeled (Figures 3C, 4A) forming a dense network of fine nerve fibers orientated parallel to the course of the corresponding circular and longitudinal muscle layers (Video S2A). The density of cholinergic fibers (hpChAT-ir) and total nerve fibers (PGP 9.5-ir) in the contoured circular and longitudinal muscle layers (Figure 4D,G, Video S2B) traced separately with Imaris 9.5 for Neuroscientists (Figure 4E,F,H,I) were denser in the circular

than in the longitudinal layer by 1.3 and 1.6 folds, respectively. However, only cholinergic fibers ($p < 0.05$) but not total nerve fibers ($p = 0.09$) reached a significant difference (Figure 5A). The percentage of hpChAT-ir in PGP 9.5-ir fibers (v/v) was 76% and 88% in the circular and longitudinal layer, respectively, without a significant difference between them ($p = 0.22$). The intensities of hpChAT and PGP9.5-ir fibers were also stronger in the circular than in the longitudinal layer by 1.5 and 1.8 folds ($p < 0.05$ and $p < 0.001$), respectively (Figure 5B).

3.2.3 | Enteric plexus—In the SMP, the intrinsic cholinergic neurons labeled by hpChAT occurred either as single cells or clustered within ganglia (Figure 6A). They were homogeneous with a small size and an eccentric nucleus. The 3D images and videos showed that intrinsic cholinergic neurons and fibers within the SMP appeared distributed in two or three layers: the ISP positioned near the mucosa and OSP located near the internal side of the circular muscle layer, as well as a third intermediate submucosal plexus (IMSP) lying between the inner and outer SMP (Figure 6B). Several images involving three layers were stitched together by using Imaris Stitcher and ganglia within each layer could be visualized in a larger field (Video S3A). These layers were connected by nerve fiber bundles coming from the submucosal intrinsic cholinergic nerve cell bodies in each layer (Figure 6B, Video S3A). In the MP, 3D images and videos exhibited a clear spatial view of the microstructures of the cholinergic nerve network in all 4 sigmoid colonic samples. The neurons were more heterogeneous and distributed in a single layer located between the longitudinal and circular muscle layers and 3 classes of hpChAT-ir nerve fiber strands (NFS) were displayed: primary NFS (NFS-I, define as the main bundle connecting the ganglia), secondary NFS (NFS-II, fibers branching out of the NFS-I) and tertiary NFS (NFS-III representing non-stranded fibers outside of NFS-I) (Figure 6C), which is consistent with a previous report on MP labeling with PGP9.5 in human descending colon.[25] Myenteric ganglia were located at the junctions of NFS-I and at the branching points of secondary nerve fiber strands. Tertiary nerve fiber strands ramified into the adjacent muscle layers (Figure 6C, Video S3B).

3.3 | Digital tracing of cholinergic process projections

In the mucosa, cholinergic cell neurites and nerve fibers labeled by hpChAT traced digitally (Figure 7A) were congregated into a local micro-network (Figure 7B). In the MP, both Dogiel type I neurons with small soma, one long and several short processes, and Dogiel type II neurons characterized by a large and smooth soma with several long processes were hpChAT-ir with labeling being stronger in type II than type I (Figure 7C). Digital tracing showed that most of processes from Dogiel type I and II neurons ran long distance and integrate into the NFS-I. A few processes just run short distance and end in the ganglion (Figure 7D,E).

3.4 | Co-localization of hpChAT and nNOS

Double labeling of hpChAT and nNOS showed a marked difference among the SMP and MP not only in the number of single-labeled hpChAT-ir and nNOS-ir neurons but also in the pattern of co-localization. In the SMP, hpChAT-ir neurons were predominantly distributed while no or a few nNOS-ir neurons were observed in the ISP (Figure 8A,D) or OSP (Figure 8B,E). In the MP, however, the two neuronal populations appeared similarly distributed

(Figure 8C,F). The computational quantitation of the soma coded in different color in 3D images of ISP (Figures 8A',D', 9D,G), OSP (Figures 8B',E', 9E,H), and MP (Figures 8C',F', 9F,I) indicated that the percentage of hpChAT-ir nerve cell bodies is significantly higher than that of nNOS-ir in total hpChAT+nNOS neurons in the ISP (98.4 ± 1.6 vs. 1.6 ± 1.6, $p < 0.001$) and the OSP (88.2 ± 5.9 vs. 11.8 ± 5.9 ($p < 0.0.01$) respectively while not different in the MP (52.9 ± 4.5 vs. 47.1 ± 4.5, $p = 0.926$) (Figure 9J). In the merged images, there was no or few co-labeled neurons found in the ISP (Figure 8G) or OSP (Figure 8H) while a remarkable co-labeling was visualized in both hpChAT and nNOS- ir neurons in the MP (Figure 8I). The percentages of co-labeled (hpChAT+nNOS) neurons in hpChAT or nNOS-ir neurons (Figure 10A–I) were 1.0 ± 1.0% or 0.0 ± 0.0% in the ISP ($p = 1$), 8.5 ± 3.5% or 70.8 ± 11.0% in the OSP ($p < 0.001$) and 30.1 ± 1.9% or 35.9 ± 6.9% in the MP ($p = 0.908$) (Figure 10J) respectively. In the hpChAT-ir neurons, the co-labeled neurons were higher in the MP than the ISP or OSP (30.1 ± 1.9 vs. 1.0 ± 1.0 or 8.5 ± 3.5, $p < 0.05$ or $p < 0.01$). In the nNOS-ir neurons, the co-labeled neurons were not found in the ISP (0.0 ± 0.0). In the OSP, they were significantly higher than the ISP or MP (70.8 ± 11.0 vs. 0.0 ± 0.0 or 35.9 ± 6.9, $p < 0.001$ or $p < 0.001$). In the MP, they were significantly higher than the ISP (35.9 ± 6.9 vs. 0.0 ± 0.0, $p < 0.001$) (Figure 10J).

4 | DISCUSSION

The present study provides new insight into the cholinergic innervation in the human sigmoid colon. This was achieved by developing a modified CLARITY protocol taking into account the unique characteristics of the sigmoid, namely a much thicker wall than other colonic segments, and abundant fat and fibrous components in the submucosa layer.[15] These features greatly extended the time required for tissue transparency and thereby increased the cross-linking and limited the hydrogel porosity thereby hampering the antibody penetration. To circumvent these issues, we increased sodium dodecyl sulfate from 4% to 6% (wt/v) in the clearing solution and separated the hydrogel hybridized full thickness of human sigmoid colon into SM and ME. We also cut vertically the hydrogel fixed full thickness specimen into thick sections (0.5–1.0 mm) for imaging the colonic innervation in all layers simultaneously. These additional steps enabled us to clear the SM and ME or the full thickness vertical section within 2 to 4 weeks rather than 6 weeks when using the intact samples. The method employed here further shortened the staining step by 3–5 days when compared to the original protocol. Moreover, an important benefit was the lowering of the clearing temperature from 55–60°C to 37°C which was particularly favorable to maintain the antigenicity and improve the immunostaining.

To demonstrate the intrinsic cholinergic innervation in the human colon, a tool labeling specifically the cholinergic fibers and terminals originating from the ENS rather than from the extrinsic innervation was an essential prerequisite. However, most antibodies raised against choline acetyltransferase (ChAT), the acetylcholine synthesizing enzyme labeling cholinergic neurons in the CNS, failed to recognize cholinergic nerves in peripheral tissues.[27–31] A leap forward occurred with the identification of a ChAT mRNA splice variant which lacks exons 6–9 in the coding region and is predominantly expressed in rat peripheral cholinergic neurons termed as peripheral form of ChAT (pChAT).[32] Little is known about the functional difference between pChAT and the well-established common form of ChAT

(cChAT).[33,34] A biochemical study in the rat primary sensory dorsal root ganglion (DRG), which contains pChAT but not cChAT, has clearly indicated that pChAT possesses ACh synthesizing ChAT activity but with only approximately 5–10% of that reported in various rat brain regions that contain cChAT but not pChAT.[35] However, despite the lower ChAT activity, the content of ACh in DRG neuronal cells is at least as high as that seen in many regions of the rat brain. Such a metabolic state appears due to a low activity of acetylcolinesterase (AChE), a degrading enzyme of ACh, detected in DRG neurons.[35] It needs to be further explored whether pChAT synthesizes ACh in cells or tissues where AChE activity is low. An in vitro molecular analysis using human embryonic kidney cells also suggested that pChAT differs from cChAT in intracellular translocation.[36] By using the antiserum against rat pChAT, peripheral cholinergic cells and fibers including those in the ENS were labeled specifically in the rat,[32,36–39] mouse,[40] guinea-pig,[33] sheep,[41,42] and pig.[34] Very recently, a novel mouse antiserum against the predicted human pChAT (hpChAT) was successfully developed and characterized to label peripheral cholinergic neurons in the human large intestine without cross-reacting with ChAT expressed in the CNS.[20] The specificity of the hpChAT antiserum for labeling of enteric cholinergic enteric neurons in human sigmoid was further confirmed in the present study by demonstrating that the immunoreactivity of hpChAT was fully colocalized with that of ChAT AB144p and P3YEB, two ChAT antibodies commonly used for immunostaining of human colonic enteric cholinergic neurons.[23,24] Importantly, the hpChAT immunostaining showed strong intensity and high sensitivity with a dilution up to 1:2000–4000 vs 1:200–500 for AB144p or 1:1000 for P3YEB and displayed more detailed structures and fine fibers with higher resolution and low background which have never been achieved before. This indicates that hpChAT antiserum is an efficient and reliable tool to assess the cholinergic innervation in the human colon. Moreover, we showed that hpChAT immunostaining is well compatible with the modified passive CLARITY technique allowing us to demonstrate for the first time the 3D features of intrinsic cholinergic innervation in each layer of the sigmoid colon.

In the mucosa, the spatial organization showed the fine intrinsic cholinergic nerve fibers which protrude into the lamina propria and surround the crypts forming a nerve network of honeycomb-like architecture. The hpChAT-ir nerve cells display Dogiel type II morphology with a smooth soma and 1–2 long processes that are distributed at the intersections of nerve fiber strands in the lamina propria. This is the first report of Dogiel type II-like neurons labeled by hpChAT in the mucosa of human sigmoid colon. Whether these neurons may act as intrinsic primary afferent neurons (IPANs) needs to be further confirmed by marker antibodies for IPANs. Taking advantage of the 3D structure and digital tracing, we could follow up the intrinsic cholinergic cell neurites and nerve fibers in the mucosa emitted from submucosal neurons. These neurites and fibers appear to be assembled into a local microneuronal network which so far has been largely unexplored in any animal species. The feature of such a rich cholinergic innervation in the mucosa may provide anatomical support for a local role to coordinate the secretion of mucus and enzymes and reabsorption of fluids in the human sigmoid colon.[43]

In the muscularis externa, 3D images showed a dense network of fine hpChAT-ir nerve fibers, which often colocalized with PGP 9.5, and ran parallel to the course of the corresponding circular and longitudinal muscle layers. Quantitative analysis showed that the

density and intensity of cholinergic fibers were significantly higher in the circular than the longitudinal muscle layer while no significant difference was detected in the density of total nerve fibers (PGP 9.5-ir) between the two layers. A previous study has quantified the cholinergic fiber density in the circular and longitudinal muscle layers in 2D images taken from 4 μm transverse sections of the human sigmoid colon. They found 47.0% of the surface area of ChAT-ir fibers labeled with an antibody against a synthetic peptide fragment of human ChAT (residues 168–189) in PGP9.5-ir fibers in both circular and longitudinal muscle.[44] In the present study, however, we found that as high as 76% and 88% of PGP 9.5-ir fibers (v/v) were stained for hpChAT in the circular and longitudinal layer, respectively. The difference may reflect the limitation of 2D imaging of thin sections and also different ChAT antibodies used for ChAT immunostaining. On the other hand, the rich intrinsic cholinergic innervation found to be denser in the circular than in the longitudinal muscle layer may indicate that ACh plays an important role in the contraction of circular muscles to move contents in contact with the mucosa to facilitate absorption (segmentation).

With regard to the SMP, the 3D images created by CLARITY combined with hpChAT staining and a rotation in a 90-degree angle allowed us to visualize the three layers, OSP, IMSP, and ISP of the human sigmoid colon. This was further illustrated, in a large field including several images with three layers stitched with Imaris Stitcher mode, by the occurrence of a couple of ganglia within each layer (Video S3A). Moreover, the 360-degree horizontal rotation of the 3D image revealed that the different layers were connected by hpChAT-ir nerve fiber bundles coming from the submucosal intrinsic cholinergic neurons in each layer. In the 2D images created from tissue sections of the human sigmoid colon, the submucosal ganglia only showed a tiered arrangement of separately identifiable plexuses,[1] which could not provide precisely and unbiasedly a spatial overview of submucosal structured due to the restriction of 2D images.

The 3D images of the MP rendered a clear spatial view with a single layer of ganglia situated between the circular and longitudinal muscle layers and an intrinsic cholinergic nerve network consisting of primary NFS-I and their two-tier branches. The intrinsic cholinergic neurons labeled by hpChAT antiserum showed Dogiel type I or II morphology. Because these images were generated within a region of 3D space and broke the durance of plane display, they allowed us to trace process projections by using Imaris program. The tracing data demonstrated that most processes of hpChAT-ir Dogiel type I and type II neurons ran into the NFS-I while a few of them just coursed short distance and ended in the ganglion. Pompolo and Furness reported that myenteric IPANs (Dogiel type II neurons) have axons that supply terminals around several types of nerve cells including other IPANs, interneurons, and motor neurons (Dogiel type I neurons) in the guinea-pig small intestine.[45]

It is well known that individual neurons express a combination of different neurotransmitters[46] in both brain and enteric neurons.[47,48] In the ENS of human colon, cholinergic and nitrergic neurons represent the major populations of excitatory and inhibitory motor neurons, respectively.[49,50] The double labeling of hpChAT and nNOS indicated distinct patterns of distribution and co-localization of these two neuronal populations among the ISP, OSP, and MP in the human sigmoid colon. Only a few or no nNOS-ir neurons were found in both ISP and OSP while hpChAT-ir neurons were

predominant. By contrast, in the MP, hpChAT-ir neurons are less in number than nNOS-ir neurons with a ratio of 1.0:1.2. The co-localization of two markers occurred in 30.1% of hpChAT-ir and 35.9% of nNOS-ir neurons in the MP. A previous study performed in other segments of the human colon reported that nerve cell bodies containing ChAT and those containing NOS occurred with a ratio of 1.0:1.2 in the MP of the ascending segment and 1.1:1.0 in the descending segment[49] that may be indicative of different gradient of excitatory and inhibitory motor neurons across colonic segments. The functional significance of the co-localization of hpChAT and nNOS within the enteric neurons and its distinct patterns among the plexuses in the human sigmoid colon remains to be clarified.

In conclusion, our modified CLARITY protocol is well suitable for clearing human colon with improved time-efficiency and beneficial for immunolabeling. By combination with novel hpChAT antiserum, 3D imaging, digital tracing and computational analysis, we demonstrated the intrinsic cholinergic innervation in different colon layers and their connections in 3D structure of the human sigmoid which could be hardly achieved in 2D images. This provides a new insight into the dense intrinsic cholinergic innervation of human sigmoid and the use of such an approach to delineate alterations under functional colonic diseases.

Supplementary Material

Refer to Web version on PubMed Central for supplementary material.

ACKNOWLEDGEMENTS

This research was supported by the NIH SPARC OT2 grant OD024899 (PQY, YT), NIHDDK Grant P30-DK-41301 (YT), Veteran Administration Research Career Scientist Award (YT), and Japan Society for the Promotion of Science KAKENHI Grant Number 18K0885300 (JPB). We thank Dr Michael Schemann for the generous supply of the ChAT (P3YEB) antibody and constructive discussion. Honghui Liang excellent technical assistance is also acknowledge.

Funding information

Japan Society for the Promotion of Science KAKENHI, Grant/Award Number: 18K0885300; NIH SPARC OT2, Grant/Award Number: OD024899; NIHDDK, Grant/Award Number: P30-DK-41301

REFERENCES

1. Hoyle CH, Burnstock G. Neuronal populations in the submucous plexus of the human colon. J Anat. 1989;166:7–22. [PubMed: 2621148]
2. Furness JB. The enteric nervous system and neurogastroenterology. Nat Rev Gastroenterol Hepatol. 2012;9:286–294. [PubMed: 22392290]
3. Furness JB, Callaghan BP, Rivera LR, Cho H. The enteric nervous system and gastrointestinal innervation: integrated local and central control. Adv Exo Med Biol. 2014;817:39–71.
4. Furness JB. Types of neurons in the enteric nervous system. J Auton Nerv Syst. 2000;81:87–96. [PubMed: 10869706]
5. Tuchin VV, Maksimova IL, Zimnyakov DA, Kon IL, Mavlutov AH, Mishin AA. Light propagation in tissues with controlled optical properties. J Biomed Opt. 1997;2:401–417. [PubMed: 23014964]
6. Tainaka K, Kubota SI, Suyama TQ, et al. Whole-body imaging with single-cell resolution by tissue decolorization. Cell. 2014;159:911–924. [PubMed: 25417165]
7. Chung K, Deisseroth K. CLARITY for mapping the nervous system. Nat Methods. 2013;10:508–513. [PubMed: 23722210]

8. Yang B, Treweek J, Kulkarni R, et al. Single-cell phenotyping within transparent intact tissue through whole-body clearing. Cell. 2014;158:945–958. [PubMed: 25088144]
9. Neckel H, Mattheus U, Hirt B, Just L, Mack AF. Large-scale tissue clearing (PACT): Technical evaluation and new perspectives in immunofluorescence, histology, and ultrastructure. Sci Rep. 2016;6:34331. [PubMed: 27680942]
10. Hama H, Kurokawa H, Kawano H, et al. Scale: a chemical approach for fluorescence imaging and reconstruction of transparent mouse brain. Nat Neurosci. 2011;14:1481–1488. [PubMed: 21878933]
11. Susaki EA, Tainaka K, Perrin D, et al. Whole-brain imaging with single-cell resolution using chemical cocktails and computational analysis. Cell. 2014;157:726–739. [PubMed: 24746791]
12. Dodt H–U, Leischner U, Schierloh A, et al. Ultramicroscopy: three-dimensional visualization of neuronal networks in the whole mouse brain. Nat Methods. 2007;4:331–336. [PubMed: 17384643]
13. Erturk A, Becker K, Jährling N, et al. Three-dimensional imaging of solvent-cleared organs using 3DISCO. Nat Protoc. 2012;7:1983–1995. [PubMed: 23060243]
14. Fung C, Tan S, Nakajima M, et al. High resolution mapping reveals that microniches in the gastric glands control Helicobacter pylori colonization of the stomach. PLoS Biol. 2019;17(5):e3000231. [PubMed: 31048876]
15. Thomson HJ, Busuttil A, Eastwood MA, Smith AN, Elton RA. The submucosa of the human colon. J Ultrastruct Mol Struct Res. 1986;96:22–30. [PubMed: 3681020]
16. Brookes SJ. Classes of enteric nerve cells in the guinea-pig small intestine. Anat Rec. 2001;262:58–70. [PubMed: 11146429]
17. Wood JD. Physiology of the enteric nervous system. In: Johnson LR, ed. Physiology of the Gastrointestinal Tract. New York: Raven; 1987:67–110.
18. Kern F Jr, Almy TP. The effects of acetylcholine and methacholine upon the human colon. J Clin Invest. 1952;31:555–560. [PubMed: 14938433]
19. Stanborough RJ. Sigmoid Colon: Where It Is, What It Does, and Why It's Important. https://www.healthline.com›health›digestivehealth›sigmoid-colon. 4 26, 2019
20. Bellier JP, Yuan PQ, Mukaisho K, Tooyama I, Tache Y, Kimura H. A novel antiserum against a predicted human peripheral choline acetyltransferase (hpChAT) for labeling neuronal structures in human colon. Front Neuroanat. 2019;13:1–15. [PubMed: 30760983]
21. Lyster DJ, Bywater RA, Taylor GS. Neurogenic control of myoelectric complexes in the mouse isolated colon. Gastroenterology. 1995;108:1371–1378. [PubMed: 7729628]
22. Lundberg LM, Alm P, Wharton J, Polak JM. Protein gene product 9.5 (PGP 9.5). A new neuronal marker visualizing the whole uterine innervation and pregnancy-induced and developmental changes in the guinea pig. Histochemistry. 1988;90:9–17. [PubMed: 2976412]
23. Giaroni C, Zanetti E, Chiaravalli AM, et al. Evidence for a glutamatergic modulation of the cholinergic function in the human enteric nervous system via NMDA receptors. Eur J Pharmacol. 2003;22:63–69.
24. Humenick A, Chen BN, Lauder CI, et al. Characterization of projections of longitudinal muscle motor neurons in human colon. Neurogastroenterol Motil. 2019;31:e13685. [PubMed: 31355986]
25. Sanders KM, Ward SM. Nitric oxide and its role as a non-adrenergic, non-cholinergic inhibitory neurotransmitter in the gastrointestinal tract. Br J Pharmacol. 2019;176:212–227. [PubMed: 30063800]
26. Lefebvre RA. Nitric oxide in the peripheral nervous system. Ann Med. 1995;27:379–388. [PubMed: 7546628]
27. Wedel T, Roblick U, Gleiss J, et al. Organization of the enteric nervous system in the human colon demonstrated by wholemount immunohistochemistry with special reference to the submucous plexus. Ann Anat. 1999;181:327–337. [PubMed: 10427369]
28. Anglade P, Larabi-Godinot Y. Historical landmarks in the histochemistry of the cholinergic synapse: perspectives for future researches. Biomed Res. 2010;31:1–12. [PubMed: 20203414]
29. Kimura H, McGeer PL, Peng F, McGee EG. Choline acetyltransferase containing neurons in rodent brain demonstrated by immunohistochemistry. Science. 1980;208:1057–1059. [PubMed: 6990490]

30. Eckenstein F, Sofroniew MV. Identification of central cholinergic neurons containing both choline acetyltransferase and acetylcholinesterase and of central neurons containing only acetylcholinesterase. J. Neurosci. 1983;3:2286–2291. [PubMed: 6355402]
31. Arvidsson U, Riedl M, Elde R, Meister B. Vesicular acetylcholine transporter (VAChT) protein: a novel and unique marker for cholinergic neurons in the central and peripheral nervous systems. J Comp Neurol. 1997;378:454–467. [PubMed: 9034903]
32. Tooyama I, Kimura H. A protein encoded by an alternative splice variant of choline acetyltransferase mRNA is localized preferentially in peripheral nerve cells and fibers. J Chem Neuroanat. 2000;17:217–226. [PubMed: 10697248]
33. Chiocchetti R, Poole DP, Kimura H, et al. Evidence that two forms of choline acetyltransferase are differentially expressed in subclasses of enteric neurons. Cell Tissue Res. 2003;311:11–22. [PubMed: 12483280]
34. Brehmer A, Schrodl F, Neuhuber W, Tooyama I, Kimura H. Coexpression pattern of neuronal nitric oxide synthase and two variants of choline acetyltransferase in myenteric neurons of porcine ileum. J Chem Neuroanat. 2004;27:33–41. [PubMed: 15036361]
35. Bellier JP, Kimura H. Acetylcholine synthesis by choline acetyltransferase of a peripheral type as demonstrated in adult rat dorsal root ganglion. J Neurochem. 2007;101:1607–1618. [PubMed: 17542812]
36. Nakajima K, Tooyama I, Yasuhara O, Aimi Y, Kimura H. Immunohistochemical demonstration of choline acetyltransferase of a peripheral type (pChAT) in the enteric nervous system of rats. J Chem Neuroanat. 2000;18:31–40. [PubMed: 10708917]
37. Yuan PQ, Kimura H, Million M, et al. Central vagal stimulation activates enteric cholinergic neurons in the stomach and VIP neurons in the duodenum in conscious rats. Peptides. 2005;26:653–664. [PubMed: 15752581]
38. Yuan PQ, Million M, Wu SV, Rivier J, Taché Y. Peripheral corticotropin releasing factor (CRF) and a novel CRF1 receptor agonist, stressin1-A activate CRF1 receptor expressing cholinergic and nitrergic myenteric neurons selectively in the colon of conscious rats. Neurogastroenterol Motil. 2007;19:923–936. [PubMed: 17973638]
39. Yuan PQ, Taché Y. Abdominal surgery induced gastric ileus and activation of M1-like macrophages in the gastric myenteric plexus: prevention by central vagal activation in rats. Am J Physiol Gastrointest Liver Physiol. 2017;313:G320–G329. [PubMed: 28684460]
40. Wang L, Martinez V, Kimura H, Taché Y. 5-hydroxytryptophan activates colonic myenteric neurons and propulsive motor function through 5-HT4 receptors in conscious mice. Am J Physiol Gastrointest Liver Physiol. 2007;292:G419–G428. [PubMed: 16990446]
41. Chiocchetti R, Grandis A, Bombardi C, et al. Characterization of neurons expressing calbindin immunoreactivity in the ileum of the unweaned and mature sheep. Cell Tissue Res. 2004;318:289–303. [PubMed: 15338268]
42. Mazzuoli G, Mazzoni M, Albanese V, et al. Morphology and neurochemistry of descending and ascending myenteric plexus neurons of sheep ileum. Anat Rec. 2007;290:1480–2149.
43. Harkins JM, Sajjad H. Anatomy, Abdomen and Pelvis, Sigmoid Colon. Stat Pearls [Internet]. Treasure Island (FL): StatPearls Publishing; 2020.
44. Golder M, Burleigh DE, Belai A, et al. Smooth muscle cholinergic denervation hypersensitivity in diverticular disease. Lancet. 2003;361:1945–1951. [PubMed: 12801738]
45. Pompolo S, Furness JB. Quantitative analysis of inputs to somatostatin-immunoreactive descending interneurons in the myenteric plexus of the guinea-pig small intestine. Cell Tissue Res. 1998;294:219–226. [PubMed: 9799437]
46. Burnstock G Do some nerve cells release more than one transmitter? Neuroscience. 1976;1:239–248. [PubMed: 11370511]
47. Chan-Palay V, Palay SL. Coexistence of Neuroactive Substances in Neurons. New York, NY: Wiley; 1984.
48. Hökfelt T, Millhorn D, Seroogy K, et al. Coexistence of peptides with classical neurotransmitters. Experientia. 1987;43:768–780. [PubMed: 2885215]

49. Wattchow D, Brookes S, Murphy E, Carbone S, de Fontgalland D, Costa M. Regional variation in the neurochemical coding of the myenteric plexus of the human colon and changes in patients with slow transit constipation. Neurogastroenterol Motil. 2008;2012:1298–1305.

50. Porter AJ, Wattchow DA, Brookes SJ, Costa M. The neurochemical coding and projections of circular muscle motor neurons in the human colon. Gastroenterology. 1997;113:1916–1923. [PubMed: 9394731]

51. Tang S, Shen C, Lin P, et al. Pancreatic neuro-insular network in young mice revealed by 3D panoramic histology. Diabetologia. 2019;61:158–167.

Keypoints

- This study developed a modified CLARITY protocol suitable for clearing of human sigmoid colon and combined with immunofluorescence using a novel mouse anti-human peripheral ChAT (hpChAT) antiserum to map the intrinsic cholinergic innervation in 3D structure of the human sigmoid colon that is little known so far.
- 3D features of intrinsic cholinergic innervation were demonstrated layer by layer in 3D images and videos which could not be displayed in 2D images.
- The density and intensity of hpChAT-ir fibers in the circular and longitudinal muscle layer and the co-localization of hpChAT and nNOS in the inner, outer submucosal, and myenteric neurons were computationally quantitated with Imaris 9.2 and 9.5.
- Data provide a new insight into the dense intrinsic cholinergic innervation of human sigmoid and the use of such an approach to delineate alterations under functional colonic diseases.

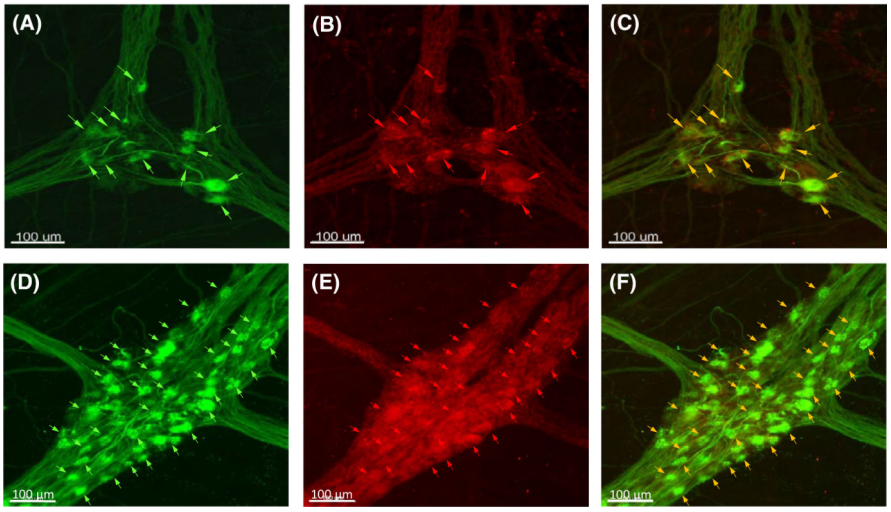

FIGURE 1.

Double labeling using a novel mouse antiserum against human peripheral choline acetyltransferase (hpChAT) combined with either one of two classic ChAT antibodies, a goat anti-human ChAT antibody (Chemicon, AB144p) or a rabbit anti-porcine ChAT antibody (Dr. Schemann, P3YEB). Confocal microscope images of myenteric plexuses of human sigmoid colon after modified passive CLARITY technique were created using Imaris 9.2 slice mode. A, D, hpChAT. B, ChAT (AB144p). E, ChAT (P3YEB). C, a merged images of A and B. F, a merged image of D and E. The arrows point to the neurons co-labeled by hpChAT and ChAT (AB144p) (upper panel) or ChAT (P3YEB) (lower panel)

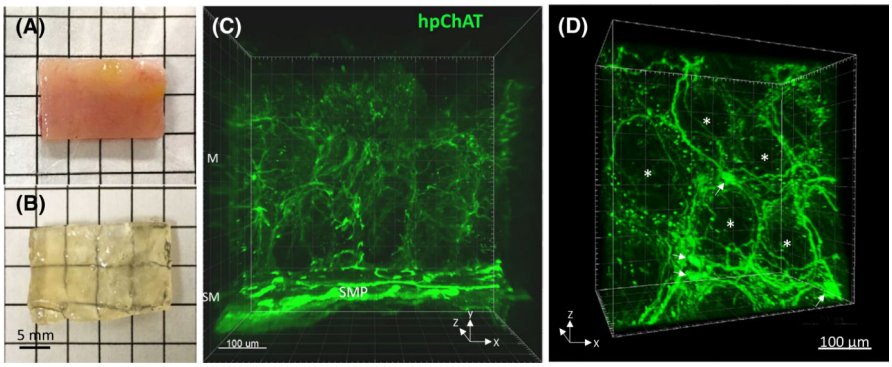

FIGURE 2.

A non-diseased sigmoid colon tissue before (A) and after (B) clearing with the modified passive CLARITY technique. The tissue-hydrogel hybrid turned transparent (B) and permeable for antibody penetration (C,D). C, A 3D image (500 µm depth scan) of the mucosa (M) and submucosa (SM) in the transparent tissue stained by immunofluorescence using a novel mouse antiserum against human peripheral choline acetyltransferase (hpChAT). Green fluorescent hpChAT-ir nerve fibers in the mucosa appeared to be projected from hpChAT-ir neurons in the submucosal plexus (SMP). A 360-degree panoramic presentation of this 3D image is shown in Video S1. D, A 3D Image in the lamina propria showing fine hpChAT-ir nerve fiber strands forming a honeycomb-like network around the mucosal crypts (*). A few nerve cell bodies (arrows) were seen at the intersections of nerve fiber strands

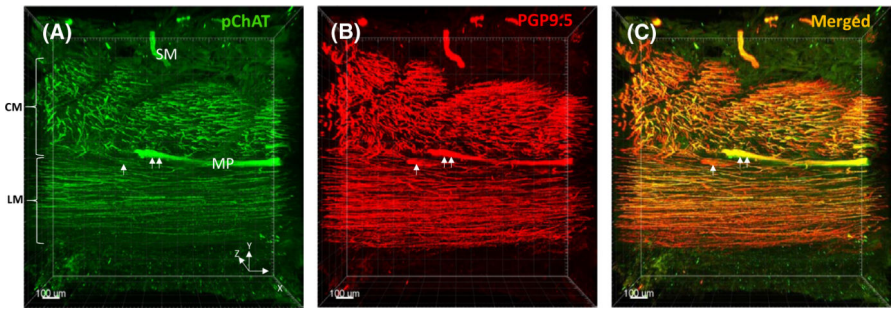

FIGURE 3.

3D images (0.5–1 mm depth scan) of the muscularis externa including layers of the circular muscle (CM), myenteric plexus (MP), and longitudinal muscle (LM) in the human sigmoid colon. A, Cholinergic nerve fiber bundles and ganglia were stained in green with mouse antiserum against human peripheral choline acetyltransferase (hpChAT). B, The same section was stained in red with protein gene product 9.5 (PGP 9.5), a pan-neuronal marker, to reveal all neuronal structures. C, A merged image showing that most of nerve fiber bundles and ganglia were labeled by hpChAT (yellow). The single arrow indicates a ganglion labeled by PGP9.5 but not hpChAT. The double arrow indicates a ganglion labeled by both hpChAT and PGP 9.5

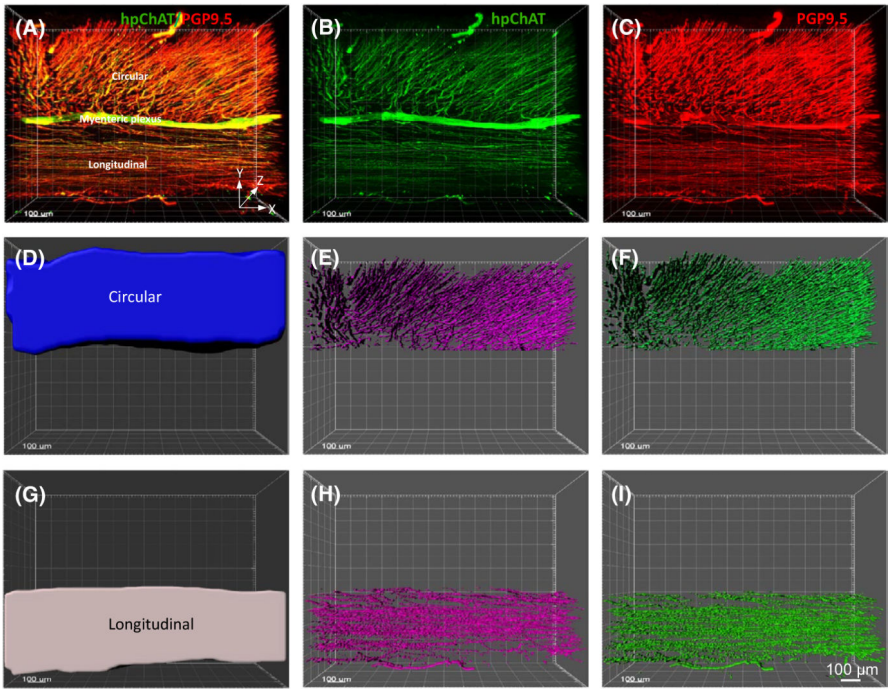

FIGURE 4.

An example of 3D images of the sigmoid colon wall with full layers used for quantifying the density and intensity of hpChAT-ir and PGP 9.5-ir fibers in the muscularis externa (ME) using Imaris 9.5 for Neuroscientists. Each 3D image was generated from 500–550 optical sections (Z-stack) with 1415 × 1415 µm frame and 1 µm apart (10× objective). A double-stained image for hpChAT-ir cholinergic and PGP 9.5-ir total nerve fibers is shown in A, while singly stained images is shown in B (hpChAT) and C (PGP 9.5). The entire circular (D) and longitudinal muscle (G) layers were contoured separately in each 3D image for measurements of their volumes. The hpChAT-ir (E, H) and PGP 9.5-ir fibers (F, I) were digitally traced to measure volumes of fibers for calculating each density and intensity. The 360-degree views of the merged image and contoured muscle layers are also shown in Video S2

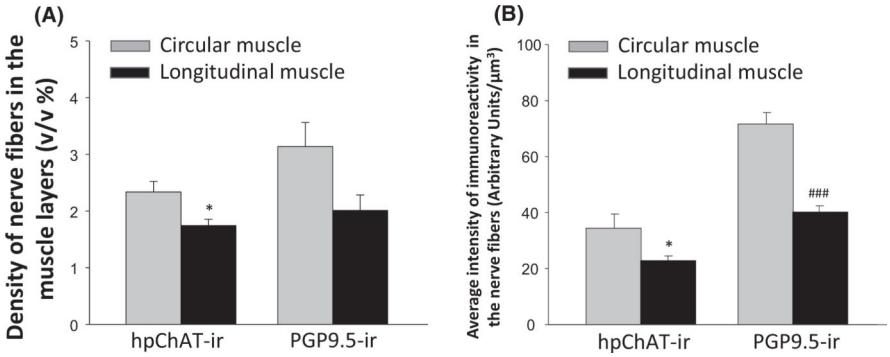

FIGURE 5.

The density (A) and intensity (B) of hpChAT-ir and PGP 9.5-ir fibers in the muscularis externa of the human sigmoid colon calculated as described in the text. Values of stained nerve fiber density are expressed as mean percentages to the volume of contoured muscle layer ($\mu m^3/\mu m^3$, %). Average values of immunofluorescence intensity are expressed as arbitrary units/μm^3. Each column represents the mean ± SEM of 3 patients. Asterisk in hpChAT-ir nerves and hashes in PGP 9.5-ir fibers respectively indicate significant difference between the two muscle layers ($^{*}p < 0.05$, $^{\#\#\#}p < 0.001$)

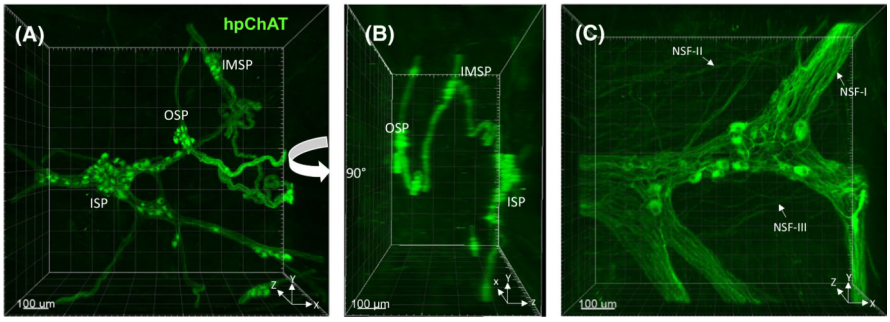

FIGURE 6.

3D images showing hpChAT-ir cholinergic neuronal cells and nerve fiber bundles in the submucosal plexus (SMP) and myenteric plexus (MP) of human sigmoid colon after passive CLARITY technique. A, Note that hpChAT-ir cells are distributed in three subplexuses of the SMP: the inner submucosal plexus (ISP), outer submucosal plexus (OSP), and the third intermediate submucosal plexus (IMSP) between the ISP and OSP. B, A side view of Figure 6A after 90° rotation shows the three ganglion layers and connecting fiber bundles in the SMP. C, A 3D image of the MP with a single layer of ganglia and an intrinsic cholinergic nerve network consisting of primary nerve fiber strands (NFS-I) and their two-tier branches (NFS-II and III) pointed by arrows. The 360-degree views of Figure 5A and C are also shown in Video S3A and B

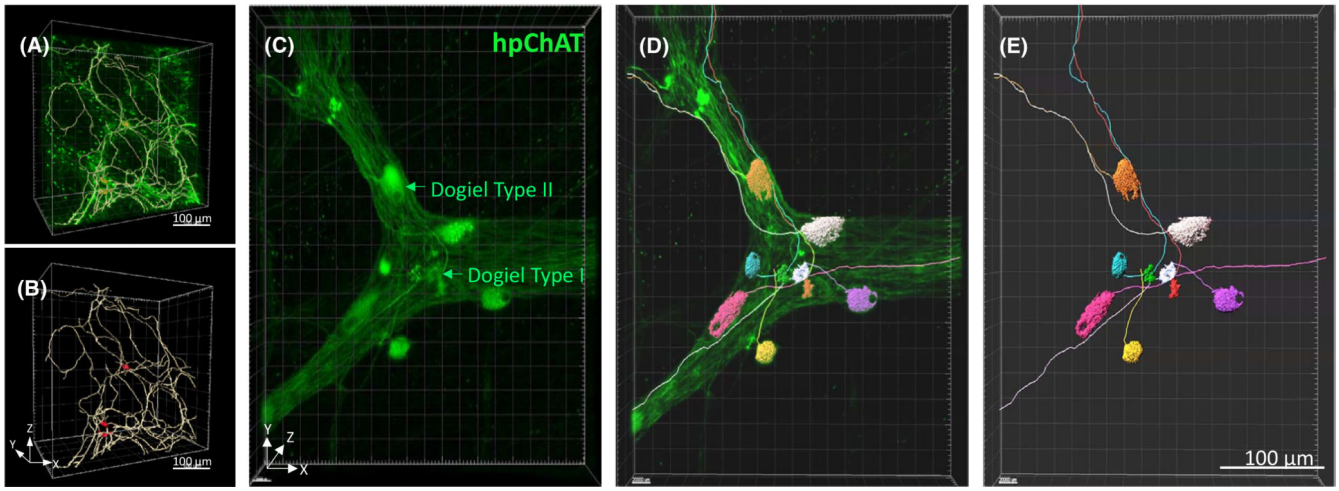

FIGURE 7.

3D imaging and digital tracing of local process projections and connectivity of hpChAT-ir cholinergic neurons in the mucosa (A,B) and myenteric plexus (C-E) of human sigmoid colon using Imaris 9.2 for Neuroscientists. Some traceable green nerve fibers, digitally yellow-labeled in A and extracted in B, show the pattern of local cholinergic network in the mucosa. The nerve cell bodies and fibers are depicted in red and yellow, respectively. C, A 3D Image shows hpChAT-ir cholinergic structures in the myenteric plexus. Both Dogiel type I neurons with small soma, one long and several short processes, and Dogiel type II neurons characterized by a large and smooth soma with several long processes are clearly stained for hpChAT, with labeling being stronger in type II than type I. D and E, Some clearly stained hpChAT-ir cell bodies and fibers in C are digitally labeled in D, and extracted in E

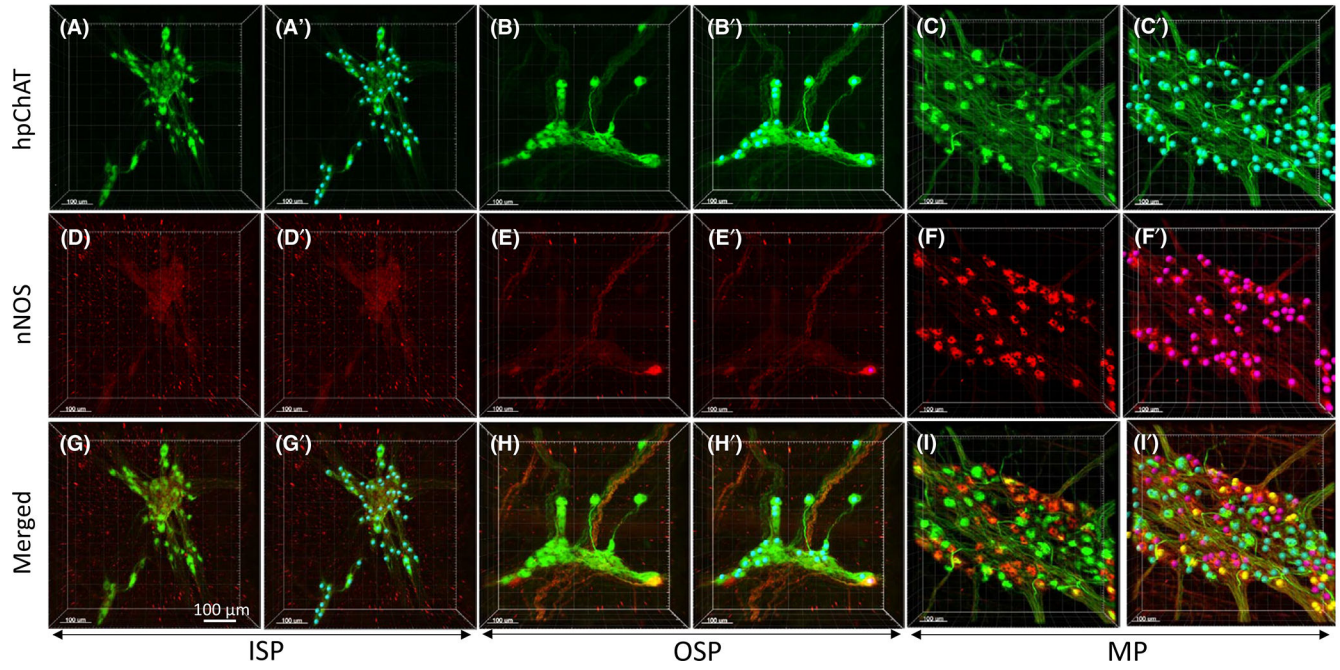

FIGURE 8.

3D images of enteric neurons in the human sigmoid colon double-labeled with a novel mouse anti-human peripheral form of choline acetyltransferase (hpChAT) and a rabbit anti-human neuronal nitric oxide synthase (nNOS) antibodies and coded with spots by Imaris 9.5 in 3D structures for computational quantitation. A, A', D, D', G, G', inner submucosal plexus (ISP). B, B', E, E', H, H', outer submucosal plexus (OSP). C, C', F, F', I, I', myenteric plexus (MP). A-C, hpChAT-ir neurons (green). D-F, nNOS-ir neurons (red). Each image in the bottom column (G-I) shows a merged image of its upper two. Cells in yellow represent co-localization of two markers. A'-C', hpChAT-ir neurons coded by blue color spots, D'-F', nNOS-ir neurons were coded by purple color spots. G'-I', Co-labeled neurons coded as yellow color by using spot function with Imaris 9'5. Scale bars: 100 µm

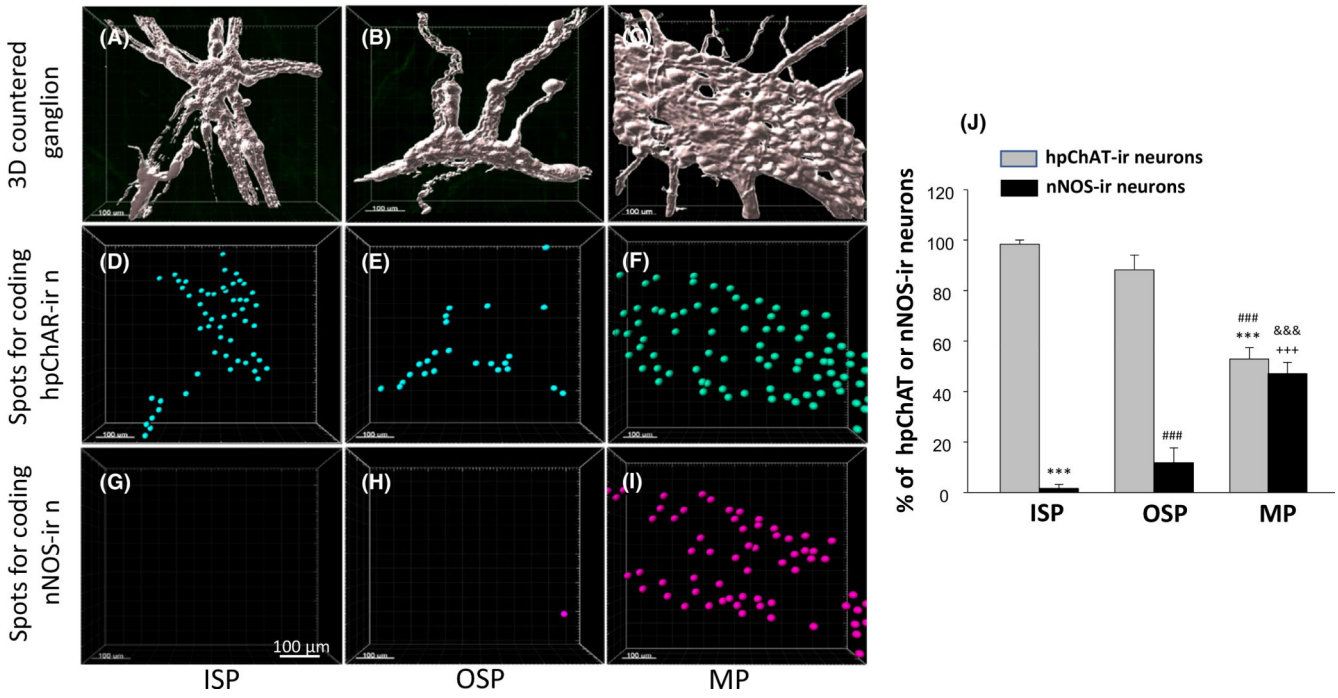

FIGURE 9.

Quantification of hpChAT-ir and nNOS-ir neurons in 3D contoured enteric ganglia (A-C) of the human sigmoid colon. A, D, G, inner submucosal plexus (ISP). B, E, H, outer submucosal plexus (OSP). C, F, I, myenteric plexus (MP). The spots for coding hpChAT (D-F in blue) and nNOS (G-H in purple) extracted from Figure 8A'-F' were counted automatically using Imaris 9.5 spot function. Scale bars: 100 µm. J, The calculation for the number of color-coded spots (hpChAT-ir or nNOS-ir) per volume of contoured ganglion (mm^3) was carried out in 4–10 ganglia of each plexus/patient and expressed as the percentage of each type of neurons in total (hpChAT+nNOS) neurons. Error bars: mean ±SEM of 3–4 patients (3 for ISP and OSP). Significant difference in number: *** or $^{###}p <$ 0.001 compared with hpChAT-ir neurons in ISP or OSP, respectively; $^{+++}$ or $^{\&\&\&}>p < 0.001$ compared with nNOS-ir neuorns in ISP or OSP, respectively

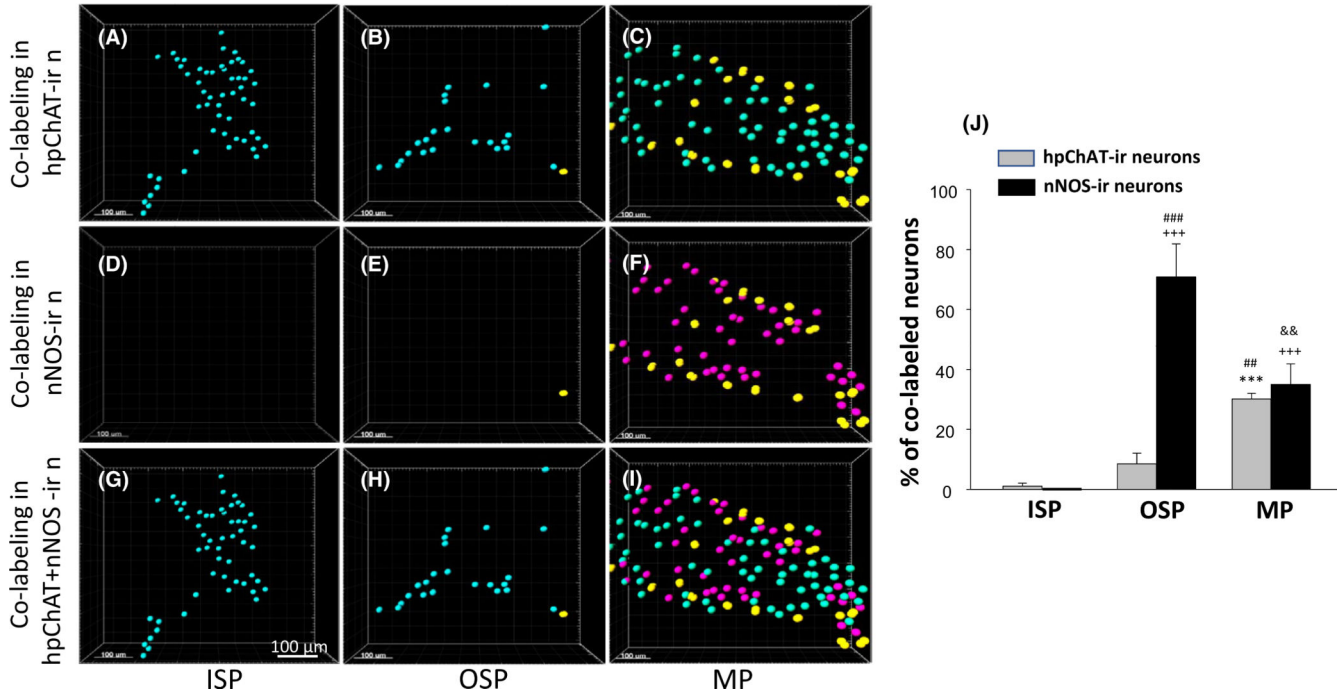

FIGURE 10.

Assessment of co-localization of hpChAT and nNOS in the preparations shown in Figure 9. The distance between each center of two different color spots was measured, using Imaris 9.5 “center point” mode, to identify co-labeled neurons being close in distance (<10.5 µm). Co-labeled spots (yellow), extracted using the ImarisColoc tool, were superimposed in hpChAT-ir (blue, A-C) or nNOS-ir (purple, D-F) spot images. A, D, G, inner submucosal plexus (ISP). B, E, H: outer submucosal plexus OSP). C, F, I, myenteric plexus (MP). The bottom images (G-I) show co-labeled neurons intermingled with both hpChAT and nNOS ones. Bars =100 µm. J, The co-localization was calculated in 4–10 ganglia of each plexus from a patient and expressed as the percentage of co-labeled neurons in hpChAT-ir or nNOS-ir neurons. Error bars: mean ±SEM of 3–4 patients (3 for ISP and OSP). Significant difference in number: *** or <0.001 or $p < 0.01$ compared with hpChAT-ir neurons in ISP or OSP, $^{###}p < 0.001$ compared with hpChAT-ir neurons in OSP, respectively; $^{+++}p < 0.001$ compared with nNOS-ir neuorns in ISP; $^{\&\&}p < 0.01$ compared with nNOS-ir neurons in OSP

TABLE 1

Immunofluorescence reagents

	Name	Immunogen	Host	Source/product no.	Dilution	Ref.
Primary antibodies	hpChAT	CSYKALLDRTQSSRK (Pat. 04412018JP, 2018)	Mouse	Dr. Bellier/H3	1:2000	[20]
	ChAT	human placental ChAT	Goat	Chemicon/AB144p	1:200–500	[23]
	ChAT	porcine ChAT peptide residues (GLFSSYRLPGHTQDTLVAQKSS)	Rabbit	Dr.Schemann/P3YEB	1:1000	[24]
	PGP9.5	human PGP9.5 peptide residues	Rabbit monoclonal	Abcam/ab108986	1:1000	[24]
	nNOS	human nNOS peptide residues	Rabbit monoclonal	Abcam/ab76067	1:1000	[51]
Secondary antibodies	Alexa 488-conjugated anti-mouse IgG	Mouse IgG (H + L)	Donkey	Jackson Imm Res/AB_2340846	1:400	
	Alexa 594-conjugated anti-goat IgG	Goat IgG (H + L)	Donkey	Jackson Imm Res/AB_2340432	1:400	
	Alexa 555-conjugated anti-rabbit IgG	Rabbit IgG (H + L)	Donkey	Abcam/ab150062	1:400	
Normal serum	Normal donkey serum	(-)	Donkey	Jackson Imm Res	1:10	